ORIENTAL JOURNAL OF CHEMISTRY
An International Open Access, Peer Reviewed Research Journal
www.orientjchem.org
ISSN: 0970-020 X
CODEN: OJCHEG
2024, Vol. 40, No.(6):
Pg. 1696-1702

In silico Analysis of 9H-(Fluorenyl) Methyl Lysine Carbamate Derivatives as Butyrylcholinesterase Inhibitors

MAHALAKSHMI C. S. PAREPALLI[1,2] and RAJITHA GALLA[2]*

[1]Department of Pharmaceutical Chemistry, G. Pulla Reddy College of Pharmacy, Mehdipatnam, Hyderabad, Telangana, India.
[2]Institute of Pharmaceutical Technology, Sri Padmavati Mahila Visvavidyalayam, Tirupati, Andhra Pradesh, India.
*Corresponding author E-mail: grajitha@spmvv.ac.in

http://dx.doi.org/10.13005/ojc/400621

(Received: October 07, 2024; Accepted: November 10, 2024)

ABSTRACT

The successful treatment strategy for Alzheimer's disease focuses on inhibiting acetylcholinesterase (AChE) and butyrylcholinesterase (BChE) to enhance cholinergic activity. This study aimed to design fifteen 9H-(fluorenyl)methyl lysine carbamate derivatives **(4a-o)** as potential BChE inhibitors and perform molecular docking studies to identify their binding sites and evaluate their binding mechanisms on the BChE protein by Glide software. The results revealed that the most potent compounds were **4a**, **4c**, and **4j**, with docking scores of -10.53, -10.57, and -10.85 kcal/mol, respectively indicating strong binding affinities with the BChE enzyme, suggesting as potential inhibitors. Notably, compound **4j** exhibited complete oral absorption, high permeability in MDCK cells, and good skin permeability. Its surface area components were within acceptable ranges. Thus, compound **4j** is proposed as a promising candidate for experimental evaluation as a BChE inhibitor.

Keywords: Alzheimer disease, Acetylcholinesterase, Butyrylcholinesterase, Molecular docking, ADME studies.

INTRODUCTION

Progressive cognitive decline and memory loss characterizes Alzheimer's disease (AD), a complex neurological disease that has a major influence on quality of life and places heavy societal and economic obligations on society as a whole[1]. Cholinergic dysfunction plays an important role in the progression of Alzheimer's disease[2]. Traditional treatment for cognitive issues have included the use of acetylcholinesterase (AChE) inhibitors such as donepezil, galantamine and rivastigmine, which function by maintaining levels of acetylcholine (ACh). The first-line treatment for Alzheimer's disease involves the use of acetylcholinesterase inhibitors[3] (Fig. 1). However, these inhibitors have dose dependant limitations and poor long-term efficacy[4].

Recent research suggests that butyryl-cholinesterase (BChE) inhibitors or mixed acetyl and butyryl cholinesterase inhibitors are more effective in treating Alzheimer's disease and have fewer side effects compared to traditional acetylcholinesterase inhibitors[5]. A promising area of study for anti-AD drugs

focuses on dual-target cholinesterase inhibitors. The enzyme butyrylcholinesterase is mainly found in the brain, plasma, and liver. Hydrolysis of ACh can be facilitated in mammalian brains by AChE and BChE. Both enzymes differ genetically, structurally, and kinetically[6]. BChE is mostly located in glial cells, whereas AChE can be found in synaptic cleft (soluble) and membranes (membrane-bound). Although BChE's precise physiological role is still unknown, recent research suggests it may have a role in the development of Alzheimer's. Notably, in the advanced stages of this condition, there is an increase in BChE activity in the brain, which contributes to the breakdown of neurotransmitter acetylcholine. The underlying concept is that the decrease in acetylcholinesterase levels is countered by an increase in butyrylcholinesterase activity, leading to more pronounced cholinergic deficits[7].

It has been suggested that a more successful therapeutic approach, particularly in the latter stages of AD, would be to simultaneously block AChE and BChE. To improve cholinergic neurotransmission, it is necessary to preserve ACh levels, and this can be accomplished by targeting both enzymes[8]. One drug that exemplifies the therapeutic promise of this strategy is rivastigmine, which is used to treat Alzheimer's disease. Rivastigmine is unique among cholinesterase inhibitors in that it can reversibly bind to and block both enzymes, leading to a rise in acetylcholine levels[9]. Furthermore, not only does BChE play a part in ACh hydrolysis, but it may also be involved in non-cholinergic pathways that contribute to the pathophysiology of Alzheimer's disease[10]. Research suggests that BChE can impact the development of Aβ plaques and is involved in controlling beta-amyloid (Aβ) aggregation. In addition, it has been suggested that BChE may modulate tau pathology and neurofibrillary tangles through its interactions with tau protein, another characteristic feature of AD[11].

Researchers are making significant efforts to identify BChE inhibitors due to the complex role BChE plays in AD. Improving therapeutic efficacy while reducing side effects is the goal to develop novel drugs that preferentially inhibit BChE or display dual AChE/BChE inhibition[12]. The belief that effective disease management requires a holistic strategy addressing all facets of AD pathogenesis is the guiding principle behind these initiatives[13].

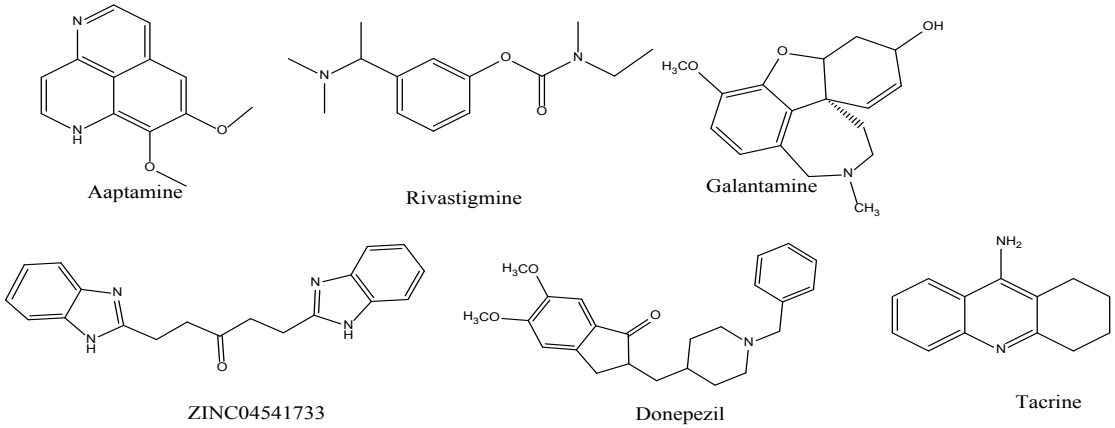

Fig. 1. Reported Cholinesterase inhibitors

Design of 9H-(fluorenyl) methyl lysine carbamate derivatives

In 1993, Tacrine (THA), a tricyclic compound became the first drug approved for treating Alzheimer's disease which act by inhibiting AChE[14]. However, by 2013, it was removed from the market due to its hepatotoxicity and gastrointestinal side effects[15].

In this study, we developed new compounds with structures similar to other tricyclic congeners, such as THA or carbazole, which are known for their cholinesterase inhibitory and neuroprotective properties. Specifically, the incorporation of Fmoc (9-fluorenyl methoxy carbonyl) significantly enhances the selectivity and stability of these compounds, establishing them as promising inhibitors of BChE[16]. Therefore, it was planned to design Fmoc-Lysine analogs that act as potent inhibitors of BChE and are well accommodated

within the active site of the enzyme thereby advancing the potential for developing therapeutic agents aimed at treating neurological disorders like Alzheimer's disease (AD) (Figure 2).

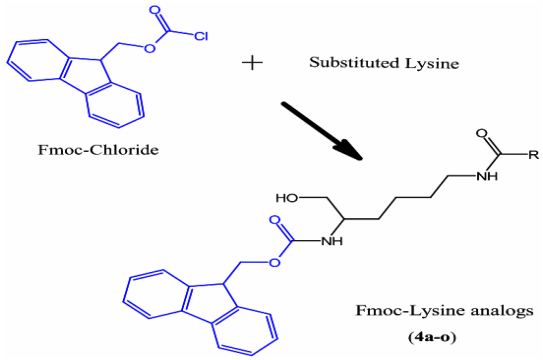

Fig. 2. Design of 9H-(fluorenyl) methyl lysine carbamate derivatives

MATERIALS AND METHODS

Docking studies

The digital structure of Human butyryl-cholinesterase (HBChE) in complex with tacrine (PDB ID 4BDS) was sourced from the protein databank[17]. The structure underwent optimization, which included the removal of unbound water molecules, the addition of hydrogen atoms to fulfill valence requirements, the incorporation of amino acids that were missed to enhance side chain stability, and energy minimization using the Protein Preparation Wizard tool from the Schrodinger Suite alongside the OPLS-2005 force field. Subsequently, the Glide Xp docking methodology was employed to investigate protein-ligand interactions with the optimized protein structure. Initially, all ligands from the dataset were docked into a three-dimensional grid designed to align with the binding pocket of target protein[18]. Binding interactions and efficiency were assessed using the Glide Score, which incorporates factors such as hydrophilic and hydrophobic interactions, Van der Waals, metal binding groups, frozen rotatable bonds, and polar interactions with receptors.

Ligand Preparation

The 2D structures of the planned derivatives were transformed into 3D using sophisticated algorithms and highly effective force fields. The Schrödinger suite's LigPrep program was used to do early geometric optimization and energy minimization on the compounds. Using the EPIK program, the LigPrep module generated a number of ionization states as well as numerous possible conformers and tautomers.

ADME Studies

The molecule descriptors and pharmaceutically relevant aspects of the results were calculated using Qikprop 4.4. that utilizes physicochemical factors to assess whether a compound possesses drug-like properties. Key factors assessed include molecular weight (MW), partition coefficient (QPlogPo/w), water solubility (QPlogS), alongside indices for intestinal absorption such as Caco-2 and MDCK permeability[19]. These comprehensive analyses facilitate the identification of compounds with optimal ADME profiles, enhancing the drug development process.

RESULTS AND DISCUSSION

Chemistry

Fifteen compounds were designed targeting the butyrylcholinesterase protein (PDB ID: 4BDS). These compounds were created by incorporating various substitutions at the carbamide moiety. The IUPAC nomenclature of designed derivatives, **4a-o** are presented in Table 1.

Molecular Docking Studies

Docking studies were conducted to predict and compare the binding mode of the target molecules with the known butyrylcholinesterase enzyme inhibitor, rivastigmine[20]. Molecular docking was utilized to evaluate possible interactions between proteins and ligands, as well as to analyze the conformational alterations of the ligands within the protein environment. The Glide XP module facilitates the generation of approximately 100 unique protein-ligand complex conformations for each docked complex, with only one being selected based on the Emodel energy. The docked compounds and co-crystal inhibitor were strategically placed within the proposed binding site of the protein to identify an optimal binding orientation. Following this, molecular docking was conducted to evaluate their binding modes and interactions with critical amino acids in the active site of the butyrylcholinesterase enzyme. The crystal structure of Human butyrylcholinesterase (HBChE) complexed with tacrine (PDB ID 4BDS) served as the basis for the initial docking model of HBChE. The successful docking of tacrine into the binding site validated the docking methodology, with rivastigmine as a reference standard.

Table 1: IUPAC nomenclature of derivatives (4a-o)

Compound	R	IUPAC Nomenclature
4a	$-C_6H_5$	(9H-fluorenyl) methyl(6-benzamido-1-hydroxyhexan-2yl) carbamate
4b	$-CH_2C_6H_5$	(9H-fluorenyl) methyl (1-hydroxy-6-(2-phenyl acetamido) hexan-2-yl) carbamate
4c	$-CH_2C_6H_5$(O-Cl)	(9H-fluorenyl)methyl(6-(2-(2-chlorophenyl)acetamido)-1-hydroxyhexan-2-yl) carbamate
4d	$-CH_2C_6H_5$(P-Cl)	(9H-fluorenyl)methyl(6-(2-(4-chlorophenyl)acetamido)-1-hydroxyhexan-2-yl) carbamate
4e	-cyclopropyl	(9H-fluorenyl)methyl(6-(cyclopropanecarboxamido)-1-hydroxyhexan-2-yl)-1-hydroxyhexan-2-yl) carbamate
4f	$-CH_2CH_3$	(9H-fluorenyl) methyl (1-hydroxy-6-propionamidohexan-2-yl) carbamate
4g	$-CH_2CH_2CH_3$	(9H-fluorenyl)methyl (6-butyramido-1-hydroxyhexan-2-yl) carbamate
4h	$-CH_2C_6H_5$(P-OCH_3)	(9H-fluorenyl) methyl (1-hydroxy-6-(2-(4-methoxyphenyl) acetamido) hexan-2-yl) carbamate
4i	$-C_6H_5$(P-Cl)	(9H-fluorenyl)methyl(6-(4-chlorobenzamido)-1-hydroxyhexan-2-yl) carbamate
4j	$-C_6H_5$(O-F)	(9H-fluorenyl)methyl(6-(2-fluorobenzamido)-1-hydroxyhexan-2-yl) carbamate
4k	$-C_6H_5$(P-Br)	(9H-fluorenyl)methyl(6-(4-bromobenzamido)-1-hydroxyhexan-2-yl) carbamate
4l	$-CH_2Cl$	(9H-fluorenyl)methyl(6-(2-chloroacetamido)-1-hydroxyhexan-2-yl) carbamate
4m	$-C_6H_5$(P-F)	(9H-fluorenyl)methyl(6-(4-fluorobenzamido)-1-hydroxyhexan-2-yl) carbamate
4n	$-C_6H_5$(O-Br)	(9H-fluorenyl)methyl(6-(2-bromobenzamido)-1-hydroxyhexan-2-yl) carbamate
4o	$-CH_2C_6H_5$(O-OCH_3)	(9H-fluorenyl) methyl (1-hydroxy-6-(2-(2-methoxyphenyl) acetamido) hexan-2-yl) carbamate

The docking analysis revealed that all compounds occupied the enzyme's active site in a manner comparable to that of tacrine. The Glide dock scores of the compounds, co-crystal ligand (tacrine) and reference standard (rivastigmine) with interacting amino acids were depicted in Table 2. The results revealed that the main interaction force of the candidate compounds, co-crystal ligand and reference standard with the HBChE active site is hydrophobic and π-π stacking interactions. All these form hydrophobic interactions with the residues (green colour) such as Val 288, Phe 329, Phe 398, Ala 199, Leu 286, Trp 231, and Ile 442. The Docking scores for all compounds varied from -6.43 kcal/mole to -10.85 kcal/mol and were found to be good inhibitors of butyrylcholinesterase. Compounds **4a**, **4c** and **4j** are more potent than the rest of the compounds. **4j** had the highest dock score of -10.851 kcal/mol, followed by **4c** (-10.57 kcal/mol) and **4a** (-10.53 kcal/mol) with binding energies -53.43, -67.47 and -61.583 kcal/mol respectively. These compounds exhibited greater potency compared to the standard drug rivastigmine, which has a docking score of -6.42 kcal/mol. The amino acids most frequently involved in Hydrogen bond with the ligands are Tyr 128, His 438, and Glu 197. Additionally, all compounds, including tacrine, interacted through π-π stacking interactions with Tyr 332, Trp 231, and Phe 329. These findings indicate that the tricyclic moiety, present in all the synthesized compounds as well as tacrine, plays a crucial role in binding to the target, which is essential for effective inhibition of the BChE enzyme. Docking interactions of **4a**, **4c**, **4j** and rivastigmine are depicted in Figure 3.

Table 2: Docking results of the compounds 4a-o

Compound	Glide Dock score(Kcal/mol)	No. of Hydrogenbonds	Amino acid residues interacted	Binding Energy(Kcal/mol)
4a	-10.53	2	Glu 197, Tyr 128	-61.583
4b	-6.57	1	His 438	-64.56
4c	-10.57	1	Tyr 128	-67.47
4d	-9.557	1	Tyr 128	-59.23
4e	-7.03	1	His 438	-56.89
4f	-9.04	3	Tyr128, Glu197, His 438	-61.052
4g	-7.23	1	His 438	-54.79
4h	-7.83	1	Glu 197	-49.76
4i	7.35	1	His 438	-60.12
4j	-10.851	1	His 438	-53.437
4k	-6.78	1	Tyr 128	-61.75
4l	-6.92	1	His 438	-64.46
4m	-7.43	0	His 438	-62.34
4n	-7.12	1	His 438	-63.12
4o	-6.43	0	His 438	-63.98
Tacrine[a]	-9.46	1	Tyr 128	-61.52
Rivastigmine[b]	-6.42	1	Gly 116	-49.275

[a]co-crystal ligand present in the human butyrylcholinesterase enzyme (PDB Id: 4BDS)
[b]reference standard drug.

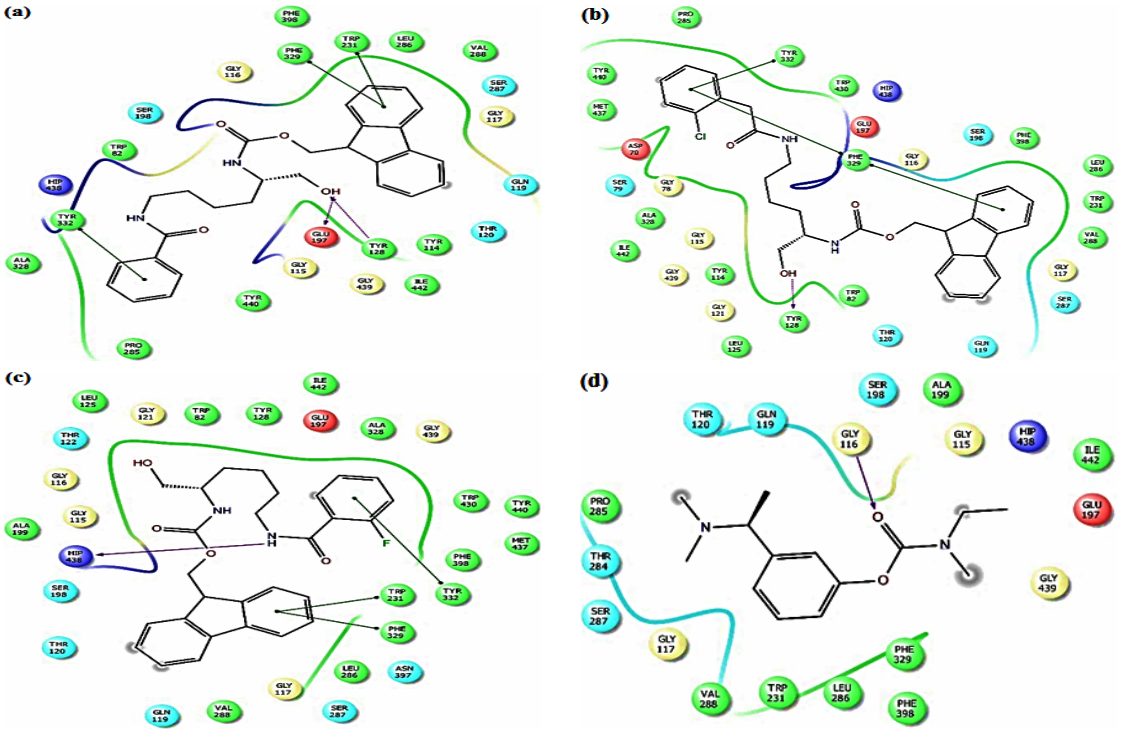

Fig. 3. 2D interaction diagrams illustrating the docked conformations of a) 4a b) 4c c) 4j and d) rivastigmine in the human butyrylcholinesterase enzyme (PDB Id: 4BDS)

ADME Molecular Properties

ADME modeling has garnered significant interest in pharmaceutical research for drug development due to its high-throughput nature and cost-effectiveness. Table 3 and Table 4 display the outcomes of molecular properties and ADME prediction produced by Qikprop for the 15 compounds. The molecular characteristics of 15 compounds were analysed, and no molecular weight violations were found. The surface area components were utilized to estimate SASA, FOSA, FISA, PISA, and volume within the recommended ranges of 300-1000, 0-750, 7-330, 0.0-450.0, and 500-2000, respectively[21]. Most of the values of **4a-o** were within the permissible range specified by Schrodinger's Qikprop guidance.

Compound permeability was predicted using the values of QPlogBB (brain-blood partition coefficient) and QPPCaco (gut-blood barrier model). A permeability score of 500 or more is considered good. Among the designed compounds, **4n** has the highest projected value, 615.777. When it comes to CNS activity, none of the substances are active. Regarding QPlogBB, each compound exhibits negative values, which suggests that they have poor permeability and are polar. According to the prediction, every compound has good skin permeability (log Kp in the -8.0-1.0 range), but only a few compounds (**4d**, **4i**, **4j**, **4k** and **4n**) have apparent MDCK cell permeability (<25: bad, >500: excellent). Almost all the compounds strongly binded to human serum albumin. (QPlogKhsa, -1.5 to +1.5) Compound **4j** demonstrated a 100% oral absorption rate (HOA) in humans, while other compounds also show a good percentage of human oral absorption.

Table 3: *In silico* prediction of molecular properties of 4a-o

Compound	MW	Dipole	SASA	FOSA	FISA	PISA	Volume
4a	458.556	0	851.772	214.554	133.632	503.585	1525.299
4b	472.583	0	873.99	251.267	133.519	489.204	1581.493
4c	507.028	0	888.318	245.024	130.687	462.428	1614.283
4d	507.028	0	898.482	251.303	133.69	441.847	1626.308
4e	422.523	0	826.835	375.166	144.74	306.929	1455.462

4f	410.512	0	792.149	353.775	136.778	301.596	1405.812
4g	424.539	0	825.167	387.05	136.527	301.59	1466.476
4h	502.609	0	922.009	349.872	135.576	436.561	1665.317
4i	493.001	0	875.839	214.554	133.638	455.994	1569.471
4j	476.546	0	856.613	213.308	129.841	479.026	1537.596
4k	537.452	0	880.853	214.546	133.629	455.275	1578.358
4l	430.93	0	783.41	270.431	140.318	301.586	1389.67
4m	476.546	0	860.811	214.554	133.636	465.597	1541.441
4n	537.452	0	871.059	210.422	127.225	471.254	1569.899
4o	502.609	0	911.675	331.785	132.083	447.807	1659.986

SASA: Solvent Accessible Surface Area, FOSA: hydrophobic component, FISA: hydrophilic component, and PISA: pi component

Table 4: *In silico* prediction of ADME profiles of 4a-o

Compound	CNS	QPlogPo/w	QPlogS	QPlogHERG	QPPCaco	QPlogBB	QPPMDCK	QPlogKp	QPlogKhsa	HOA (%)
4a	-2	5.353	-7.216	-7.941	535.387	-1.673	251.81	-1.152	0.823	94.167
4b	-2	5.062	-6.459	-6.518	311.811	-1.738	252.481	-1.105	0.607	88.264
4c	-2	5.446	-6.98	-6.422	341.365	-1.589	508.331	-1.147	0.693	78.259
4d	-2	5.555	-7.212	-6.401	312.702	-1.592	620.762	-1.275	0.721	78.214
4e	-2	3.983	-6.004	-5.647	272.643	-1.81	193.739	-2.05	0.316	93.857
4f	-2	3.735	-5.322	-5.38	309.24	-1.653	233.79	-1.922	0.199	93.385
4g	-2	4.106	-5.732	-5.536	311.894	-1.75	235.178	-1.821	0.307	95.627
4h	-2	5.2	-6.745	-6.496	275.863	-1.884	240.516	-1.232	0.638	75.159
4i	-2	5.842	-7.947	-7.821	535.32	-1.526	621.63	-1.32	0.935	96.014
4j	-2	5.558	-7.451	-7.828	581.592	-1.545	625.184	-1.169	0.855	100
4k	-2	5.918	-8.06	-7.841	535.426	-1.518	668.532	-1.322	0.958	84.517
4l	-2	3.883	-5.427	-5.338	253.679	-1.448	527.095	-2.083	0.202	92.716
4m	-2	5.587	-7.578	-7.803	535.342	-1.569	455.653	-1.286	0.864	95.535
4n	-2	5.874	-7.823	-7.825	615.777	-1.455	641.567	-1.148	0.939	85.347
4o	-2	5.209	-6.738	-6.44	327.512	-1.812	261.186	-1.128	0.63	76.549

QPlogHERG: predicted IC_{50} value for the inhibition of HERG potassium channels. QPPMDCK: predicted permeability of MDCK cells in nanometers per second

CONCLUSION

In conclusion, this study focuses on the advancement of selective inhibitors of butyrylcholinesterase (BChE), an enzyme involved in the development of Alzheimer's disease. A series of fifteen 9H-(fluorenyl) methyl lysine carbamate derivatives **(4a-o)** were rationally developed and tested using in silico procedures. Among the compounds, **4j** had the highest potency, with a docking score of -10.851 kcal/mol. Furthermore, ADME research demonstrated that compound **4j** had 100% oral absorption rate, great permeability in MDCK cells, and good skin permeability. The surface area properties, including SASA, FOSA, FISA, PISA, and molecular volume, all fell within the required range. These findings indicate that compound **4j** is a promising candidate among the series of designed compounds and can be explored further for Alzheimer's disease treatment.

ACKNOWLEDGEMENT

The authors would like to acknowledge the G. Pulla Reddy College of Pharmacy, Hyderabad and the Institute of Pharmaceutical Technology, Sri Padmavati Mahila Visvavidyalayam, Tirupati for providing a favourable research environment and supplying the necessary resources to successfully complete the work.

Conflict of interest

The authors declared no conflict of interest.

REFERENCES

1. Kinney, J. W.; Bemiller, S. M.; Murtishaw, A. S.; Leisgang, A. M.; Salazar, A. M.; Lamb, B. T., *Translational Research & Clinical Interventions.*, **2018**, *4*, 575-90.
2. Scheltens, P.; Blennow, K.; Breteler, M. M.; De Strooper, B.; Frisoni, G. B.; Salloway, S., Van der Flier, W. M., *The Lancet.*, **2016**, *388*(10043), 505-17.

3. Özdemir, Z.; Yılmaz, H.; Sarı, S.; Karakurt, A.; Şenol, F. S.; Uysal, M., *Med. Chem. Res.*, **2017**, *26*, 2293–2308.
4. Pathan A., *NeuroPharmac Journal.*, **2023**, *12*, 11-17.
5. Jasiecki, J.; Targoşska, M.; Wasąg, B., *International Journal of Molecular Sciences.*, **2021**, *22*(4), 2033.
6. Miao, S.; He, Q.; Li, C.; Wu, Y.; Liu, M.; Chen, Y.; Qi, S.; Gong, K., *Pharm Biol.*, **2022**, *60*(1), 1502-1510.
7. Pozzi, F. E.; Conti, E.; Appollonio, I.; Ferrarese, C.; Tremolizzo, L., *Front Neuroscience.*, **2022**, *16*, 998224.
8. Marucci, G.; Buccioni, M.; Dal Ben, D.; Lambertucci, C.; Volpini, R.; Amenta, F., *Neuropharmacology.*, **2021**, *190*, 108352.
9. Nguyen, K.; Hoffman, H.; Chakkamparambil, B.; Grossberg, G. T., *Neurodegenerative Disease Management.*, **2021**, *11*(1), 35-48.
10. Chen, R.; Li, X.; Chen, H.; Wang, K.; Xue, T.; Mi, J.; Ban, Y.; Zhu, G.; Zhou, Y.; Dong, W.; Tang, L., *European Journal of Medicinal Chemistry.*, **2023**, *251*, 115253.
11. Gadhave, K.; Kumar, D.; Uversky, V. N.; Giri, R., *Medicinal Research Reviews.*, **2021**, *41*(5), 2689-745.
12. Kumar, V.; Saha, A.; Roy, K., *Computational Biology and Chemistry.*, **2020**, *88*, 107355.
13. Vellom, D. C.; Radic, Z.; Li, Y.; Pickering, N. A.; Camp, S.; Taylor, P., *Biochemistry.*, **1993**, *32*(1), 12–17.
14. Radic, Z.; Pickering, N. A.; Vellom, D. C.; Camp, S.; Taylor, P., *Biochemistry.*, **1993**, *32*(45), 12074–12084.
15. Berg, L.; Andersson, C. D.; Artursson, E.; Hornberg, A.; Tunemalm, A. K; Linusson, A.; Ekstrom, F., *PLoS One.*, **2011**, *6*(11), e26039.
16. Gonzalez, J.; Ramirez, J.; Schwans, J. P., *Amino Acids.*, **2016**, *48*(12), 2755-2763.
17. Li, S.; Li, A. J.; Travers. J.; Xu, T.; Sakamuru, S.; Klumpp-Thomas, C.; Huang, R.; Xia, M., *SLAS Discov.*, **2021**, *26*(10), 1355-1364.
18. Srikanth, R.; Sivarajan, A.; Venkatesan, C. S.; Maheshwaran, V.; Sugumar, P.; Rajitha, G.; Varalakshmi, J. C.; Ponnuswamy, M. N., *Journal of Molecular Structure.*, **2016**, *1125*, 481-492.
19. Umesh, H. R.; Ramesh, K. V.; Devaraju, K. S., *J. Basic and Applied Sciences.*, **2020**, *9*, 1-4.
20. Tong, X.; Li, X.; Ayaz, M.; Ullah, F.; Sadiq, A.; Ovais, M.; Shahid, M.; Khayrullin, M.; Hazrat, A., *Front. Pharmacol.*, **2021**, *11*, 580069.
21. Divya, P.; Prasad, S. V. U. M.; Raghavendra, N. M., *Chemistry Select.*, **2023**, *7*(47), e202204248.